原著

Fundamental Examination of SPECT Images using Digital Phantom for Physical Performance Evaluation

Seiji KAWAMURA

Department of Radiological Science, Faculty of Health Science, JUNSHIN GAKUEN University

Summary(Abstract): After we did a fundamental examination of single photon emission computed tomography (SPECT) images using Prominece Processor (Prominence), software for digital phantom and nuclear medicine image processing, we report as follows. In this respect there are few studies using both filtered back projection (FBP) and ordered subsets expectation maximization (OSEM) methods for the digital phantom.

First we reconstructed the SPECT images by FBP and OSEM for the digital phantom. The present study was made for (1) cutoff frequencies by different pre-treatment filtering, (2) partial volume effects, (3) spatial resolution by different collimators, and (4) evaluation of spatial resolution by different rotary radii. We made the above evaluations by making visual evaluation, conducting measurement of counts, and calculating full width at half maximum (FWHM) and normalized mean square error (NMSE).

As a result, (1) by visual evaluation, OSEM images were shown to be stable. (2) OSEM showed lower values in the optimal cutoff frequency using NMSE. (3) The digital phantom for physical performance evaluation showed clearer, partial volume effect. (4) FWHM showed slightly lower values in FBP images. These results were found to correspond well with those of phantom experiments using radiopharmaceuticals and those of clinical SPECT images.

From the above findings, it was suggested that the digital phantom was considerably excellent in deepening the understanding of the effect of SPECT image reconstruction by FBP and OSEM on the image quality.

Keyword： OSEM, MLEM, FBP, subset, iteration, NMSE

1. Introduction

In recent years, there has become a relatively fewer involvement of radiologists in processing work of SPECT image reconstruction than in the past, which makes it increasingly difficult to have a complete understanding of the processed contents.

From the above situations, We believe it is thought to be very important to understand the effect of SPECT image reconstruction processes using personal computer (PC) and different reconstruction methods on the images. Consequently, we made a basic examination on the effect of digital phantom (http://www.jsrt.or.jp/92nm/dp/eng/download.htm) as well as FBP and OSEM image reconstruction methods using Prominece Processor [1-4], software of nuclear medicine image processing and on the usefulness of digital phantom, and we report hereunder:

2. Materials and Methods

We employed the above-mentioned digital phantom as the image reconstruction data of SPECT images. The digital phantom was developed to confirm and evaluate the fundamental performance and the reconstruction process of SPECT. The digital phantom was made by the Monte Carlo simulation EGS 4 that was based on the shape shown in the Fig. 1. As the items of evaluation, density (contrast, partial volume effect), position resolution, uniformity, etc. were able to be evaluated.

On the left side of the Fig. 1, the whole image of digital phantom was shown. For the upper part of the phantom, the rod region for examining the density (contrast, partial volume effect) and the position

Received. January 6. 2014.
Department of Radiological Science,
Faculty of Health Sciences, JUNSHIN GAKUEN University
Professor

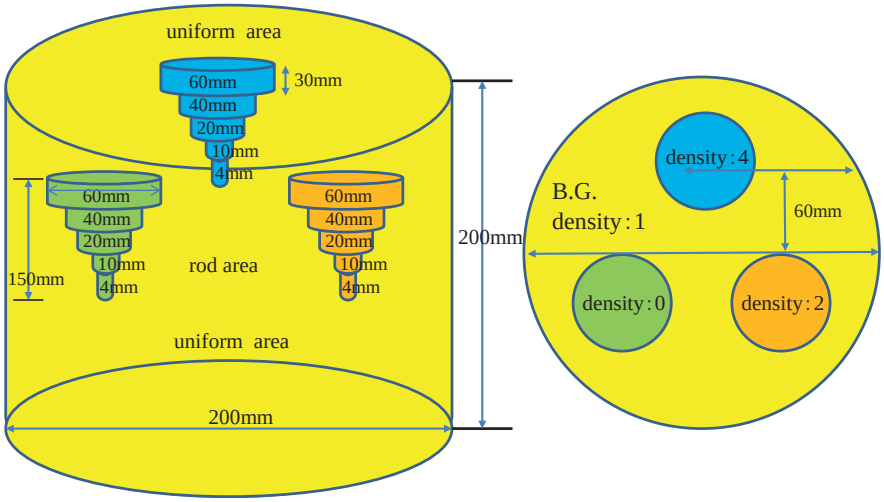

Fig.1 Schema of a digital phantom for SPECT evaluation.

resolution was provided. As shown on the right side of the Fig. 1, the setting of each count was prepared in the rod region at (0, 2, 4) with the density of the background region as 1. I, in the bottom part of the digital phantom, the uniform count domain with the density of 1 for the uniformity evaluation was provided.

For the denomination of collimator in the digital phantom, we used 2 kinds of "HR_150_4mm_3d_100" and "HR_200_4mm_3d_100" for a low energy high resolution, and "GP_200_4mm_3d_100" for a general-purpose use of a low energy. The values in the denominations of the collimator described each of the following conditions, respectively. 150 of "HR_150_4mm_3d_100" stands for a rotary radius of the detector, 4 mm means a pixel size, 3d shows the projection step angle, and 100 stands for the maximum count. For radionuclide, Tc-99m (a single photon peak of 140 keV) was set. The allowable incident angle of HR collimator was 2.5°, and that of GP collimator was 3.6°, while the energy resolution was fixed at 10%, but the specific resolution of the detector was not taken into consideration. For the purpose of comparison with the digital phantom, ideal SPECT projection data "Proj4mm_3deg_i_M.sps" and SPECT tomography data "IdealS14mm_i.sts" were provided, in which "no deterioration of the position resolution, no diffusion, no absorption, and no statistical noise due to the aperture of the collimator were observed.

2-1 Evaluation of Cut off Frequency

We applied different image reconstruction methods (FBP, OSEM) to "HR 150_4mm_3d_100" of the digital phantom to examine the differences in the images due to the cutoff frequencies and the optimal cutoff frequency, visually and by way of NMSE[5-6]. The conditions for the image reconstruction were as follows:

Range of reconstructed slices: 7~55

Reconstruction Conditions: Pre-treated filter Butterworth, order 8, cutoff 0.2~0.9 cycles/mm

Reconstruction: FBP (Ramp), OSEM ; (diffusion, attenuation, non-corrected resolution)

Data Processing Device: Prominence Processor (Windows 7 PC)

2-2 Evaluation of Partial Volume Effect

We applied different reconstruction methods (FBP, OSEM) to "HR 200_4mm_3d_100", "HR 150_4mm_3d_100" and "GP 200_4mm_3d_100" of the digital phantom to examine the partial volume effects.

At each rod region (60 mm, 40 mm, 20 mm, 10 mm, 4 mm) of the digital phantom shown in the Fig. 1, we set ROI and calculated the average count in ROI. For evaluation, we drew a graph by plotting the count of each rod that was normalized by the count in ROI with

the radius of 60 mm. We used Ideal as an ideal data platform.

2-3 Evaluation of Resolution by Different Collimators and Reconstruction Methods

We applied different reconstruction methods (FBP, OSEM) to "HR 200_4mm_3d_100", and "GP 200_4mm_3d_100" of the phantoms to examine and evaluate the resolution due to different collimators and reconstruction methods, using profile curves and FWHM.

2-4 Evaluation of Spatial Resolution by different rotary radii and reconstruction methods (FBP, OSEM)

We applied different reconstruction methods (FBP, OSEM) to "HR 200_4mm_3d_100", and "HR 150_4mm_3d_100" of the phantoms to examine and evaluate the spatial resolution due to different rotary radii and reconstruction methods, using profile curves and FWHM.

3. Results

3-1 Comparison of Images and NWSE at each Cutoff Frequency

We showed the images of the digital phantom and the value of NMSE at each cutoff frequency in Fig. 2

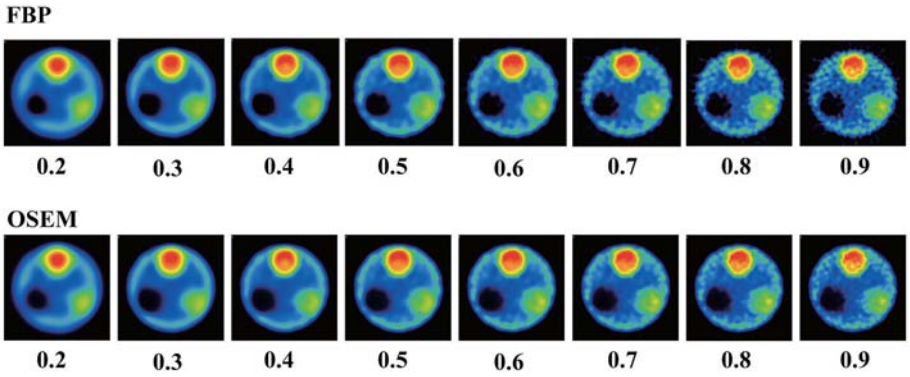

Fig. 2 This showed the images of the digital phantom at each cutoff frequency(cycles/cm)
"Collimator : HR150-4mm-3d-100 "

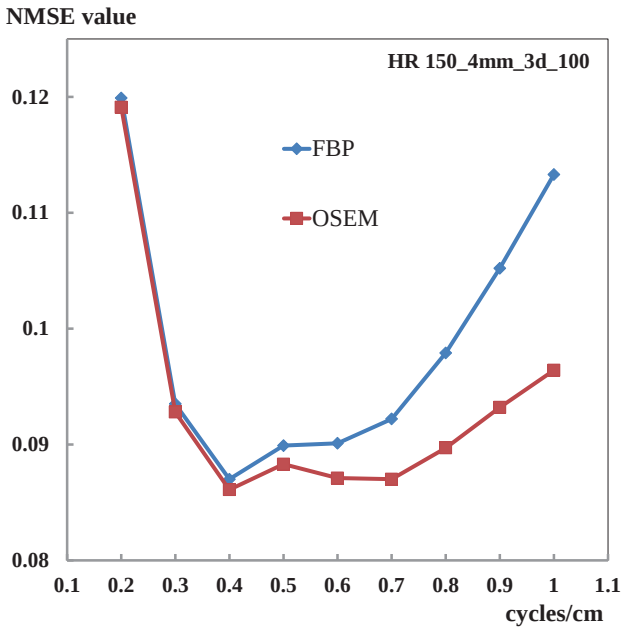

Fig. 3 Comparison of NMSE value of each cutoff frequency.

and Fig. 3 respectively. For both FBP and OSEM, a smoothing effect was well observed visually at low-cutoff frequencies. On the other hand, increased level of image noise at lower cutoff frequencies was observed. Visually, good images were shown in the range of 0.4~0.5 cycles/cm for FBP and in the range of 0.4~0.6 cycles/cm for OSEM. Also, for both FBP and OSEM, NMSE showed the minimum value at 0.4 cycles/cm. Furthermore, OSEM, compared with FBP, showed lower NMSE in wider ranges. In both visual manner and NMSE, a similar evaluation was obtained.

3-2 Partial Volume Effect using Different Reconstruction Methods and Different Collimators

Fig. 4 shows the counts after normalization of each rod in case of the use of different reconstruction methods and collimators. To the left of Fig. 4, the OSEM method was shown, and to the right the FBP method was shown. A similar tendency was observed in FBP method and OSEM methods, but with a rod radium of 10 mm, OSEM showed a more decreased, although slightly, partial volume effect.

3-3 Evaluation of Resolution by Different Collimators and Reconstruction Methods (FBP, OSEM)

Table 1 shows each rod radius and FWHM that is

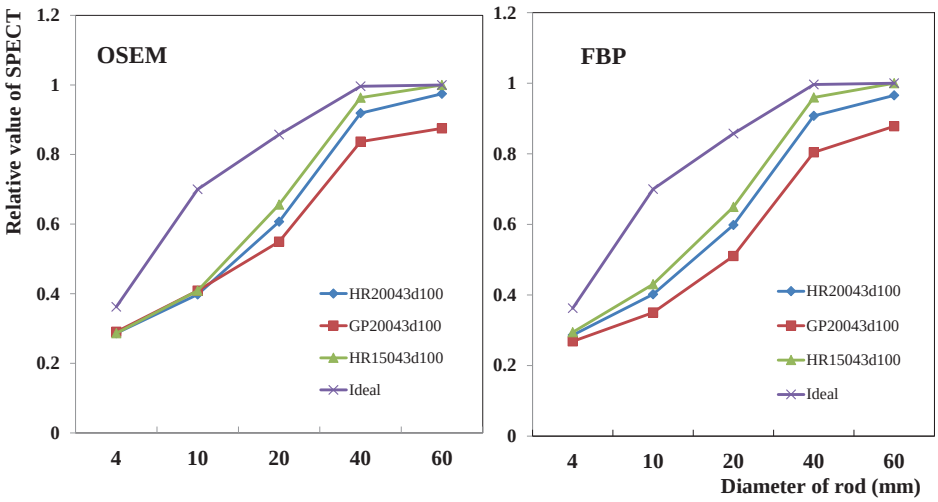

Fig. 4 Relative values that were normalized by the counts in the rod region at 60 mm

Table 1 Evaluation of FWHM resolution by different collimators and reconstruction methods

	FBP HR200-4-3d-100			
	slice	4 (r.c.)	2 (r.c.)	0 (r.c.)
60mm	8	64.3mm	79.1mm	61.3mm
40mm	15	46.0mm	67.4mm	43.4mm
20mm	23	42.8mm	○	16.2mm
10mm	30	○	△	△
4mm	38	×	×	×

	OSEM HR200-4-3d-100			
	slice	4 (r.c.)	2 (r.c.)	0 (r.c.)
60mm	8	64.1mm	79.5mm	63.8mm
40mm	15	45mm	67.6mm	44.6mm
20mm	23	44.5mm	○	20.8mm
10mm	30	○	×	×
4mm	38	×	×	×

	FBP GP200-4-3d-100			
	slice	4 (r.c.)	2 (r.c.)	0 (r.c.)
60mm	8	63.7mm	75.3mm	54.5mm
40mm	15	47.6mm	74.2mm	40.5mm
20mm	23	55.7mm	○	○
10mm	30	○	△	△
4mm	38	×	×	×

	OSEM GP200-4-3d-100			
	slice	4 (r.c.)	2 (r.c.)	0 (r.c.)
60mm	8	64.2mm	82.1mm	62mm
40mm	15	48.3mm	76.3mm	48.2mm
20mm	23	53.1mm	○	13.8mm
10mm	30	○	×	×
4mm	38	×	×	×

Table 2 Evaluation of FWHM due to different rotary radius and reconstruction methods

	FBP HR200-4-3d-100			
	slice	4 (r.c.)	2 (r.c.)	0 (r.c.)
60mm	8	64.3mm	79.1mm	61.3mm
40mm	15	46.0mm	67.4mm	43.4mm
20mm	23	42.8mm	○	16.2mm
10mm	30	○	△	△
4mm	38	×	×	×

	OSEM HR200-4-3d-100			
	slice	4 (r.c.)	2 (r.c.)	0 (r.c.)
60mm	8	64.1mm	79.5mm	63.8mm
40mm	15	45mm	67.6mm	44.6mm
20mm	23	44.5mm	○	20.8mm
10mm	30	○	×	×
4mm	38	×	×	×

	FBP 60mm HR150-4-3d-100			
	slice	4 (r.c.)	2 (r.c.)	0 (r.c.)
60mm	8	64.2mm	81mm	61.3mm
40mm	15	45mm	67.5mm	41.15mm
20mm	23	34.5mm	○	21.5mm
10mm	30	△	×	×
4mm	38	×	×	×

	OSEM 60mm HR150-4-3d-100			
	slice	4 (r.c.)	2 (r.c.)	0 (r.c.)
60mm	8	63.5mm	76.4mm	66.4mm
40mm	15	44.05mm	67.4mm	43.9mm
20mm	23	40.55mm	○	23.25mm
10mm	30	△	×	×
4mm	38	×	×	×

the resolution of each count when different collimators and different reconstruction methods were used. "HR200_4mm_3d_100" collimator showed smaller FWHM than the "GP200_4mm_3d_100" collimator. Also, FBP, compared with OSEM showed smaller, although slightly, FWHM. "○" and "△" in Table 1 stand for the ability to visually confirm rods, but the inability to calculate FWHM. "×" shows the inability to visually detect rods and to calculate FWHM.

3-4 Evaluation of Spatial Resolution due to Different Rotary Radius and Reconstruction Methods (FBP, OSEM)

Table 2 shows each rod radius and resolution of FWHM of each count when different rotary radius and different reconstruction were employed. With the rotary radius of 150 mm, compared with that of 200 mm, FWHM showed a slightly smaller value.

4. Discussion

Up to now, studies on the comparison of OSEM reconstruction algorithm, etc. among processing devices, using the digital phantom, have been conducted and published[7-10]. However, there are few studies, in which both FBP and OSEM were used, examining the effect of partial volume effect as well as different collimators and rotary radius on the resolution. Thus, in this present study, we examined, using the digital phantom, (1) evaluation of cutoff frequency related to different reconstruction methods, (2) partial volume effect, (3) evaluation of resolution due to different collimators, (4) evaluation of resolution by rotary radius and usefulness of the digital phantom.

We made a SPECT reconstruction by FBP and OSEM for "HR 150_4mm_3d" that was one of the projection data of the digital phantom, and evaluated the reconstruction in relation to "Ideal S14mm_i.sts" that was an ideal SPECT tomography, using NMSE. As a result, we found that both of the reconstruction methods showed 0.4 cycles/mm as the optimal cutoff frequency. However, despite the same projection data, OSEM showed a wider range of frequency in NMSE that was closer to the optimal cutoff frequency, as shown in Fig. 3, which was also visually observed in the images shown in the Fig. 2. Again, at 0.8 and 0.9 cycles/mm of cutoff frequency, the deterioration of FBP images, compared with that of OSEM, was clearly shown.

The partial volume effects of OSEM to the left in Fig. 4 and of FBP to the right in this Fig. 4 were shown, which indicated a similar trend. However, at

the rod radius of 10 mm, OSEM showed a slightly more reduced, partial volume effect. Although its reason is not known, it is thought that OSEM may be more appropriate for the reconstruction in a region of lower counts[11-15]. Theoretically, in comparison between HR collimator and GP collimator, GP collimator whose spatial resolution is worse is larger in the partial volume effect, and GP collimator increases its partial volume effect under the influence of deteriorated resolution at the time when the rotary radius is large. As seen above, the use of the digital phantom clearly showed the partial volume effect reduced the count values in the rod when the rod radius of either FBP or OSEM became smaller. Therefore, the digital phantom can be considered to be a very useful tool in making medical students and the beginners of nuclear medicine tests to understand the partial volume effect.

Moreover, although the differences of collimators and those of rotary radius, using the digital phantom, were expressed in terms of FWHM in Table 1 and Table 2, the differences in reconstruction was clearly shown, in which FBP, compared with OSEM, by way of collimators, showed higher contrast. However, we were unable to clearly show the differences of rotary radius in the present digital phantom, which may be attributed to the fact that the setting of the rotary radius of digital phantom was made at 150mm and 200mm. For this issue, it will be necessary to confirm it by changing the rotary radius, using the actual digital phantom, in which radionuclides are contained.

5. Conclusion

By using the digital phantom and the Prominence, software for image processing of nuclear medicine, we made a SPECT image reconstruction by OSEM and FBP, and made a comparative examination on the differences in image quality by the reconstruction methods, by way of visual way and by using the indexes such as FWHM, NMSE, etc.

- The optimal cutoff frequency using NMSE showed the same 0.4 cycles/cm for both FBP and OSEM. OESM, compared with FBP, showed a wider range of 0.4~0.7 cycles/cm with lower NMSE values.
- It was thought that the digital phantom was a useful phantom in the deepening understanding of partial volume effect, as it was possible to clearly show the partial volume effect.
- FBP showed a slightly lower value in evaluation of FWHM by different collimators.
- The digital phantom did not clearly show the differences in rotary radius.
- The digital phantom seems to be an excellent numerical phantom, making it possible to show the differences in image reconstruction of FBP and OSEM.

References

1. Hisato M, Noriyasu Y, Makoto A, et al. Development of the Software Package of the Nuclear Medicine Data Processor for Educationand Research. Jpn. J. Radiol. Technol. Vol.68, No.3, pp.299-306, 2012.
2. Seiji K, Yuuki M, Takeyuki H, et al. Study on the use order of subsets in OSEM Method. Journal of Junshin Gakuen University. pp.49-55, 2012
3. Yokoi T, Shinohara H, Onishi H. Performance evaluation of OSEM reconstruction algorithm incorporating three-dimensional distsance-dependent resolution compensation for brain SPECT:a simulation study. Ann Nucl Med ., 16(1), 11-18, 2002
4. Maeda H, Yamaki N, Natsume T, et al. Simultaneous spatial resolution correction in SPECT reconstruction using OS-EM algorithm. Igaku Butsuri., 24(2), 61-71, 2004
5. penny BC, King MA, Schwinger R, et al.: Constrained leastsquares restoration of nuclear medicine images:selecting the coarseness function. Med Phys., 14, 849-858, 1987
6. Hideo Ohnishi, Noritoshi Ushio, Matuo Satoru, et al.: Optimized Butterworth Filter for ^{99m}Tc Myocardial Perfusion SPECT images; an evaluation. Jpn. J. Radiol. Technol. Vol.52, No.3, pp.346-350, 1996
7. Koichi OGAWA, Masahiro TAKAHASHI, "Selection of projection Sets and the Order of Calculation in Ordered Subsets Expectation Maximization Method," IEICE D-Ⅱ Vol. J82-D-Ⅱ No.6 pp.1-93-1099, 1999
8. J. Li, R.J. Jaszczak, J. Li, K.L. Greer, and R.E. Coleman, "Implementation of an accelerated iterative algorithm

forcone-beam SPECT," Phys. Med. Biol., vol.39, pp.643-653, 1994.

9. Norikazu Matutomo, Hiroaki Furuya, Taichirou Yamao, Norimi Nishiyama, Takefumi Suruga, Shuichi Sugino, Shuuji Fujihara, Ryuji Yoshioka,"Comparison of OS-EM Reconstruction Algorithms among Different Processors Using a Digital Phantom Dedicated for SPECT Data Evaluation," Jpn.J.Radiol.Technol. Vol.64, No.11, pp.1361-1368, 2008.
10. Palacio M, Reducing radiation dose. Applied Radiology2010; p.4-7. http://www.appliedradiology.com/uploadedFiles/Issues/2010/12/Supplements/AR_12-10_Philips_Palacio01.pdf
11. Shepp LA, Vardi Y. Maximum likelihood reconstruction for emission tomography. IEEE Trans. Med. Imaging, MI-1. 1982; 113-122.
12. Lange K, Carson R.EM reconstruction algorithms for emission and transmission tomography. J. Compt. Assist. Tomogr. 1983; 8: 306-316.
13. Y.Vardi, L.A.Shepp, and L.Kaufman, "A statistical model for positron emission tomography," J. Amer. Statist. Assoc., vol.80, pp.8-37, 1985.
14. K.Lange, M.Bahn, and R. Little, "A theoretical study of some maximum likelihood algorithms for emission and transmission tomography," IEEE Trans. Med. Imag., vol.6, pp.106-114, 1987.
15. H.M. Hudson and R.S. Larkin, "Accelerated image reconstruction using ordered subsets of projection data," IEEE Trans. Med. Imag., vol.13, pp.601-609,1994.